2016

Extending Link Pivot Offset Optimization to Arterials with Single Controller Diverging Diamond Interchange

Christopher M. Day
Purdue University, cmday@purdue.edu

Steven M. Lavrenz
Purdue University, slavrenz@ite.org

Amanda L. Stevens
INDOT, amilynn1107@yahoo.com

R Eric Miller
INDOT, rumiller@indot.in.gov

Darcy M. Bullock
Purdue, darcy@purdue.edu

Extending Link Pivot Offset Optimization to Arterials with Single Controller Diverging Diamond Interchange

Christopher M. Day*
Purdue University
550 Stadium Mall Drive
West Lafayette, IN 47906
(765) 496-9601
cmday@purdue.edu

Steven M. Lavrenz
Purdue University
550 Stadium Mall Drive
West Lafayette, IN 47906
(765) 496-7314
slavrenz@purdue.edu

Amanda L. Stevens
Indiana Department of Transportation
8620 E. 21st St.
Indianapolis, IN 46219
(317) 796-2661
astevens@indot.in.gov

R. Eric Miller
Indiana Department of Transportation
5333 Hatfield Rd
Fort Wayne, IN 46808
(260) 969-8231
rumiller@indot.in.gov

Darcy M. Bullock
Purdue University
550 Stadium Mall Drive
West Lafayette, IN 47906
(765) 494-2226
darcy@purdue.edu

*Corresponding author.

Word Count: 4978 words + 10 * 250 words/(figure-table) = 4932 + 2500 = **7432** words

November 13, 2015

ABSTRACT

Deployments of diverging diamond interchange (DDI) have increased in recent years. Most research has focused much effort on optimizing signal timing within the DDI, but there remains a need to optimize a DDI within an existing system to ensure smooth corridor operation. This paper presents a methodology for optimizing offsets on a corridor including a single-controller DDI. This methodology uses high-resolution controller data and an enhancement to the link-pivot algorithm that deconstructs the single-controller parameters into equivalent offset adjustments. The methodology is demonstrated by its application to a 5-intersection arterial route including a DDI, and the outcomes are assessed by measurement of travel times by Bluetooth vehicle re-identification. A user benefit methodology is applied to the travel time data that considers the reliability of the travel times in addition to the central tendency. Further, the methodology is applied to O-D paths that travel to and from the freeway in addition to routes along the arterial. A total annualized user benefit of approximately $564,000 was achieved. The paper concludes by discussing how the method can also be applied to other nontraditional control schemes connected to arterials, such as continuous-flow intersections and TTI four-phase diamonds.

INTRODUCTION

The diverging diamond interchange (DDI), also known as the double crossover diamond, was first introduced in North America about 12 years ago (*1*), and has been gaining increasing acceptance as a treatment for interchanges of surface streets with limited access highways. Reversing the direction of traffic flow on the arterial lanes through the interchange eliminates the need for left turn movements that cross traffic. Consequently, the interlocked left turns in a conventional diamond can be eliminated.

DDI signal timing is more nuanced than suggested by the simplicity of the crossover intersections. The two arterial through movements are not concurrent, making them challenging to coordinate, similar to challenges with intersections that are split phased or interchanges with TTI "four phase" operation (*2*). Also, the clearance time for the crossing arterial movements is smaller than that of the ramp movements. Accommodating longer ramp clearance time requires careful controller programming that must be reconciled with other operational goals.

The Missouri Department of Transportation constructed the first DDI in the US (*3*). Timings were devised from field observations. The DDI was operated by a single controller. The crossover intersections were independently operated using one ring for each, with an offset between the rings. Clearance phases were used to achieve additional ramp red clearance times for the crossing and ramp movements.

Several researchers have explored improvement of DDI signal timing. Hu (*4*) tested several different methodologies for optimization and considered impacts under fixed-time and actuated control. Yang *et al*. (*5*) investigated a bandwidth-based model for optimizing a DDI, along with neighboring intersections. Tian *et al*. (*6*) presented six different schemes for DDI operation with variations on phase and overlap assignment and sequencing. Hainen *et al.* (*7*) investigated optimization of the offset within the DDI, and compared the operation of the existing "two-phase" operation with an alternative "three-phase" scheme that delayed the release of ramp vehicles to synchronize their arrivals at the next intersection.

The research has considered a variety of options for operating the DDI itself. However, there has been little published research regarding coordination with adjacent intersections. Schroeder *et al.* (*8*) modeled DDIs along corridors, but the study focused on model calibration rather than signal timing. The bandwidth-based solution proposed by Yang *et al.* (*5*) achieved improvements over external software only when considering the DDI as an isolated system. This may have been because incorporating the DDI into a larger system forces the DDI to operate under the system cycle length. A method is needed to optimize the signal timing of DDIs within existing coordinated systems.

This paper presents an offset-optimization methodology for arterials including single-controller interchanges, as applied to a five-section arterial with a DDI. The methodology systematically optimizes the offsets throughout the corridor, incorporating the offset within in the single-controller interchange. The outcomes are assessed not only for paths along the arterial but for other important O-D pairs as well.

STUDY OVERVIEW

Location

SR 1 (Dupont Rd.) and Interstate 69 in Fort Wayne, Indiana is the first DDI to be constructed in the state. The interchange was formerly a conventional diamond. Construction was completed in November 2014. Figure 1 shows a map of the five-intersection study corridor, which includes the DDI and three neighboring intersections. The second and third intersections comprising the DDI are operated by a single controller. The other intersections are conventional intersections operated using a phasing scheme based on the common "dual-ring, eight-phase" template (i.e., four critical phases). Intersections 1 and 5 lack side street left-turn phases. Hospitals to the north of Parkview Plaza Drive and south of Longwood Drive are major traffic generators, in addition to the arterial and freeway destinations. The numbered rectangles in Figure 1 show the locations where Bluetooth sensors were deployed to measure travel times.

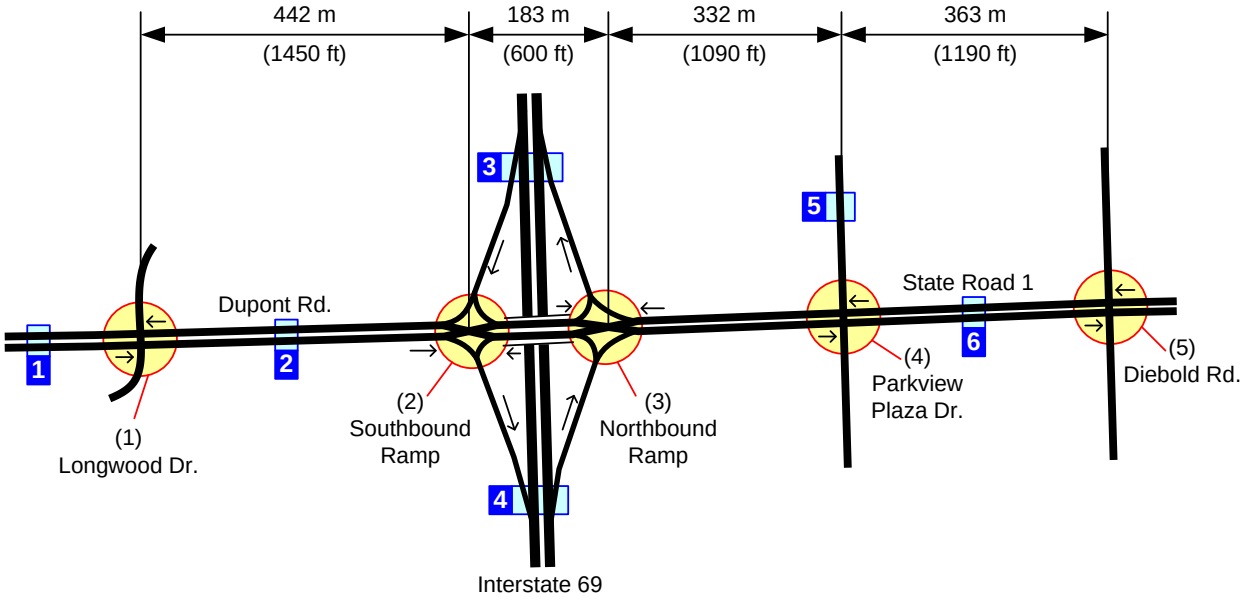

Figure 1. Map of the five-intersection study corridor: SR 1 (Dupont Rd) and Interstate 69 Exit 316, Fort Wayne, Indiana. The numbered rectangles represent location of Bluetooth monitors for travel time data collection.

Figure 2a shows the phase assignments at the DDI. Similar to previous examples (3,7), the ramp exits are controlled by even-numbered phases, while the crossover movements are operated by overlaps. Each crossover overlap includes one even-numbered and one odd-numbered parent phase.

Figure 2b explains the need for different clearance times. Consider the transition from the westbound through to the eastbound through at the crossover intersection. When the westbound through ("a") terminates, two distances must clear. The red-shaded region ("b") must clear before vehicles depart from the eastbound crossover ("c"). The orange shaded region ("d") must *additionally* clear before vehicles depart from the ramp right turn ("e"). The ramp left turn has a similar requirement, as well as the ramp phases at the other crossover intersection.

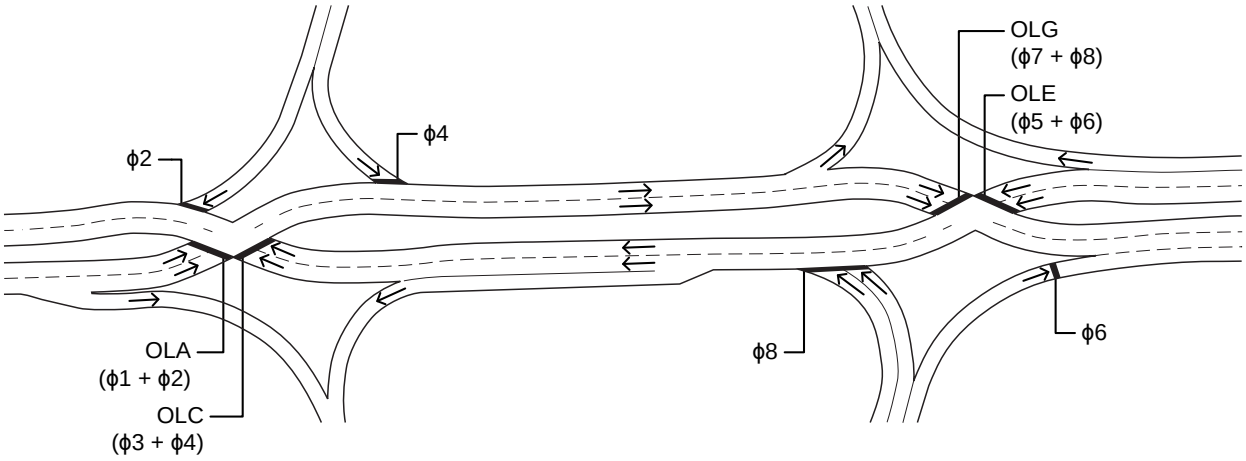

(a) Geographic layout of the SR 1 and I-69 interchange.

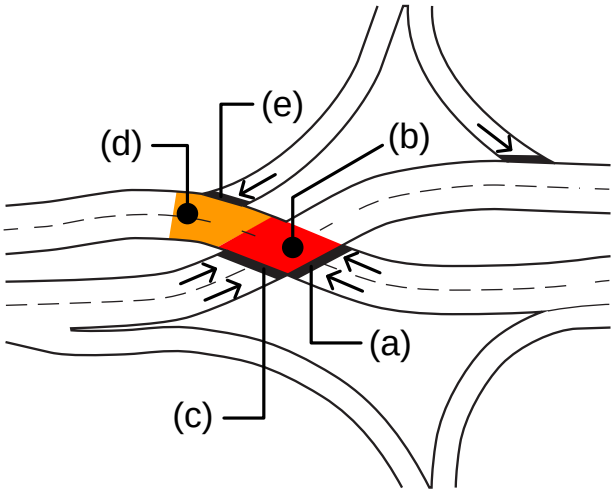

(b) Detailed view of the west intersection showing clearance distances.

Figure 2. DDI interchange geometry.

Figure 3 illustrates the phase sequence and overlap assignments in a ring diagram. Ring 1 controls the west intersection, while ring 2 controls the east intersection. Each ring controls one intersection independently, while the *ring displacement* creates a relationship between the two rings. The use of a single controller eliminates the possibility of coordination failures within the interchange, even if the rest of the system loses communication. In this example, a ring displacement is illustrated that favors eastbound movement. One can easily imagine this being reversed; thus, the ring displacement parameter could potentially be adjusted to suit the needs of traffic.

The odd-numbered phases delay the start of green for the ramp movements, achieving the required longer clearance time. For example, at the west intersection, overlaps A and C alternate in a simple "two-phase" manner. The odd-numbered clearance phases last only a few seconds; because they are not used for any field display, the short green and yellow times do not cause malfunction monitor unit errors.

The corridor operates at cycle lengths ranging from 120 to 140 seconds, depending on the time of day. The timing plan is divided into AM (0600-0830), midday (0830-1445), and PM (1445-1830) periods. The DDI crossover intersections operate at half the system cycle length; in a separate study, this was found to yield lower intersection delay than full cycle length (*9*). The clearance phases are served for 4 seconds each. Initial splits and offsets were initially obtained from Synchro, followed by manual field tuning, following agency timing practices.

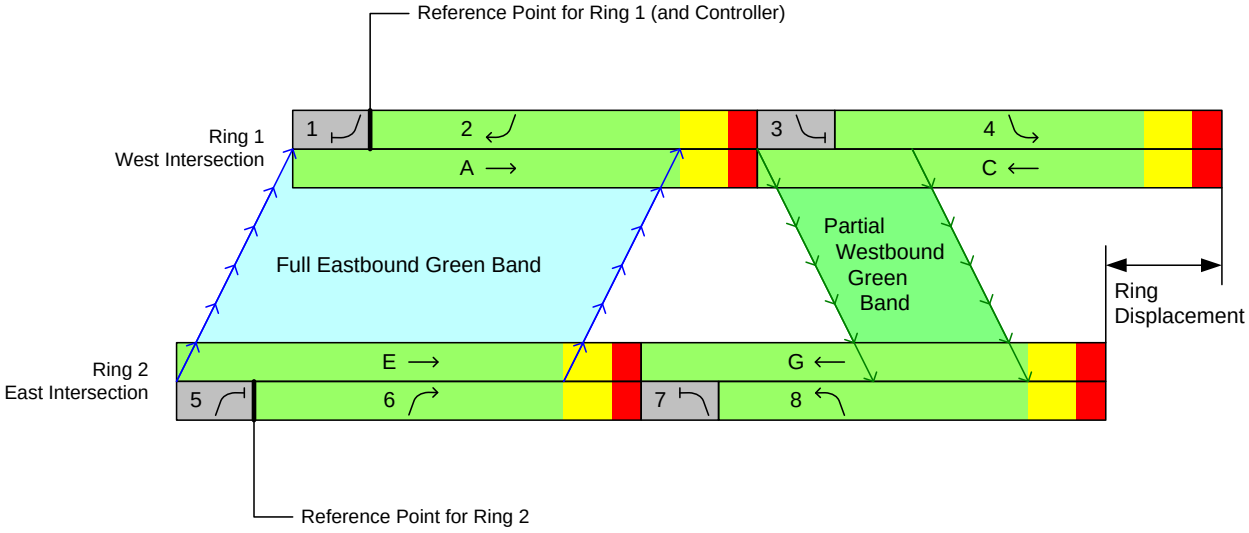

Figure 3. Ring diagram showing the sequencing of phases at the SR 1 and Interstate 69 interchange, under a hypothetical value of ring displacement.

METHODOLOGY

Data Collection

To evaluate and optimize the offsets in the corridor, high-resolution event data collection (*10,11*) was introduced. The existing controllers were upgraded to newer units with data logging capability. Cellular IP modems were used to remotely retrieve data from Ints. 1–4 using a fully automated process (*12*). At the time, it was not possible to deploy a modem at Int. 5. Instead, a small form factor computer (*13*) was placed in the cabinet to locally download the data, which was manually retrieved and inserted into the TMC server as needed.

To independently assess outcomes, travel times were measured between points in the corridor using Bluetooth MAC address matching. The locations of the Bluetooth sensors are shown in Figure 1. The arterial endpoints and freeway ramp locations enabled the measurement of travel times along the arterial, as well as for O-D paths to and from I-69.

Traffic Data Observations

Figure 4 and Figure 5 show detailed views of the quality of progression by approach using a visualization called the "Purdue Coordination Diagram" (PCD), which compares vehicle arrivals with green intervals temporally (*14*). Time in cycle flows vertically while successive cycles cascade horizontally. Moving upward within each cycle's column, the horizontal axis is the previous end of green; the green line is the beginning of green; and the upper red line is the subsequent end of green. The green-shaded area represents the green interval. Each dot marks a vehicle arrival. Gray dots show vehicles originating from upstream *turning* movements while black dots show upstream *through* movements, as determined from the status of the upstream signal at their projected time of departure (*15*). Figure 4 shows the status of each approach before optimization for a representative day from 6:00–18:30, while Figure 5 shows zoomed-in detail around 12:00–12:30 for the four approaches at the DDI crossover intersections.

Several observations can be made regarding the traffic patterns in the system:

- *Entering Movements*. Int. 1 eastbound (Figure 4a) and Int. 5 westbound (Figure 4j) show only gray dots because there was no information about the upstream signal. The arrivals are random at Int. 5, but well-formed platoons are evident at Int. 1.

- *Between Intersections 1 and 2*. Int. 1 westbound (Figure 4b) features two platoons because the upstream DDI crossover intersection is half cycled. Few turning vehicles are in the stream. Meanwhile, Int. 2 Eastbound (Figure 4c) has the appearance of completely random arrivals when zoomed out, but the detailed view (Figure 5a) shows that the arrivals actually exhibit a repeating two-cycle pattern that occurs due to half cycling.

- *Within the DDI*. The two through movements exiting the DDI are Int. 2 westbound (Figure 4d, Figure 5b) and Int. 3 eastbound (Figure 4e, Figure 5c). As is typical of diamond interchanges, well-formed platoons are observed at the interchange exiting movements. Int. 3 eastbound is exceptionally well-timed during the PM peak, but during the rest of the day the arrivals appear early. Int. 2 westbound shows substantial room for improvement during all three time of day patterns.

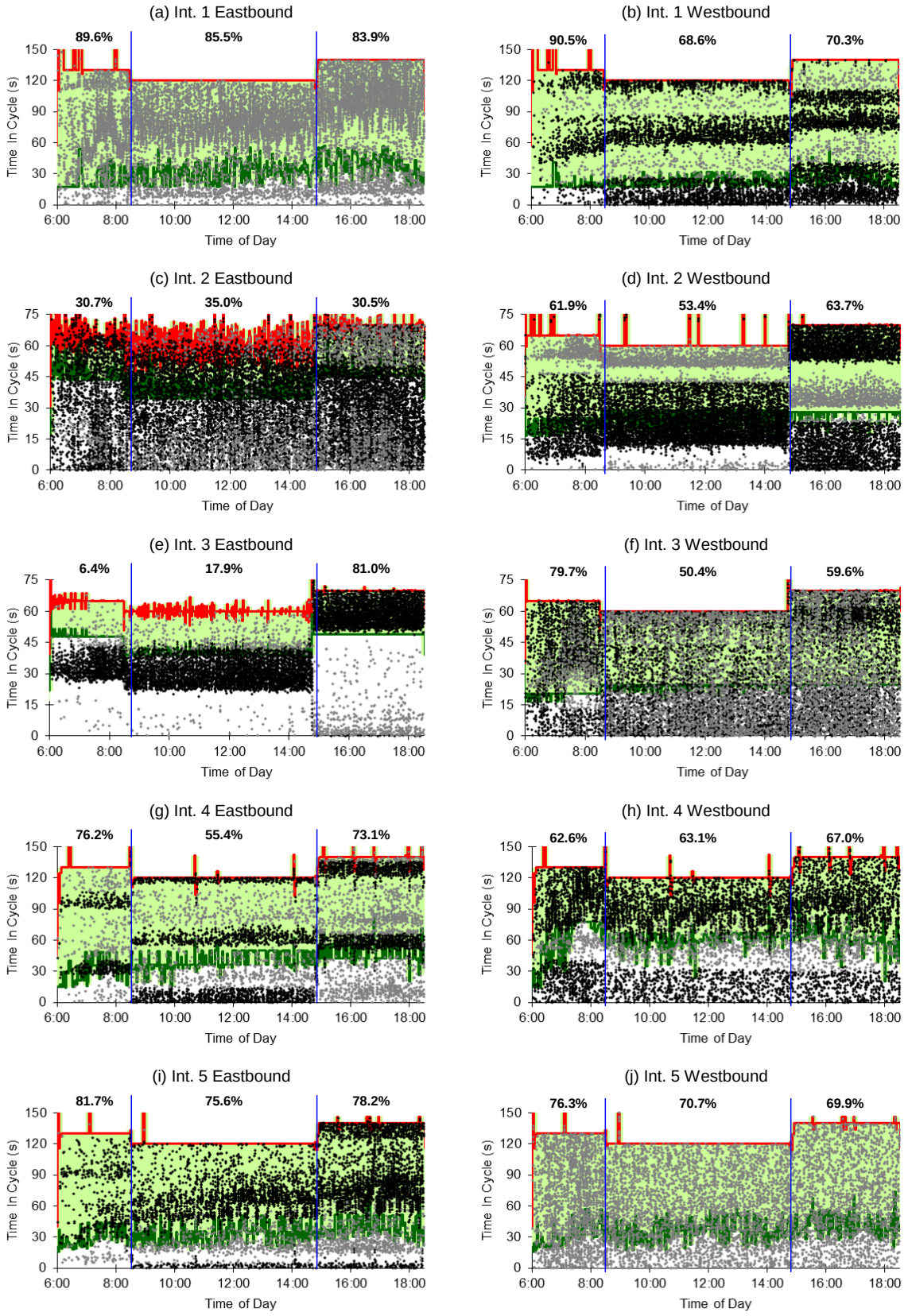

Figure 4. PCDs for Wednesday, May 6, 2015 (before optimization).

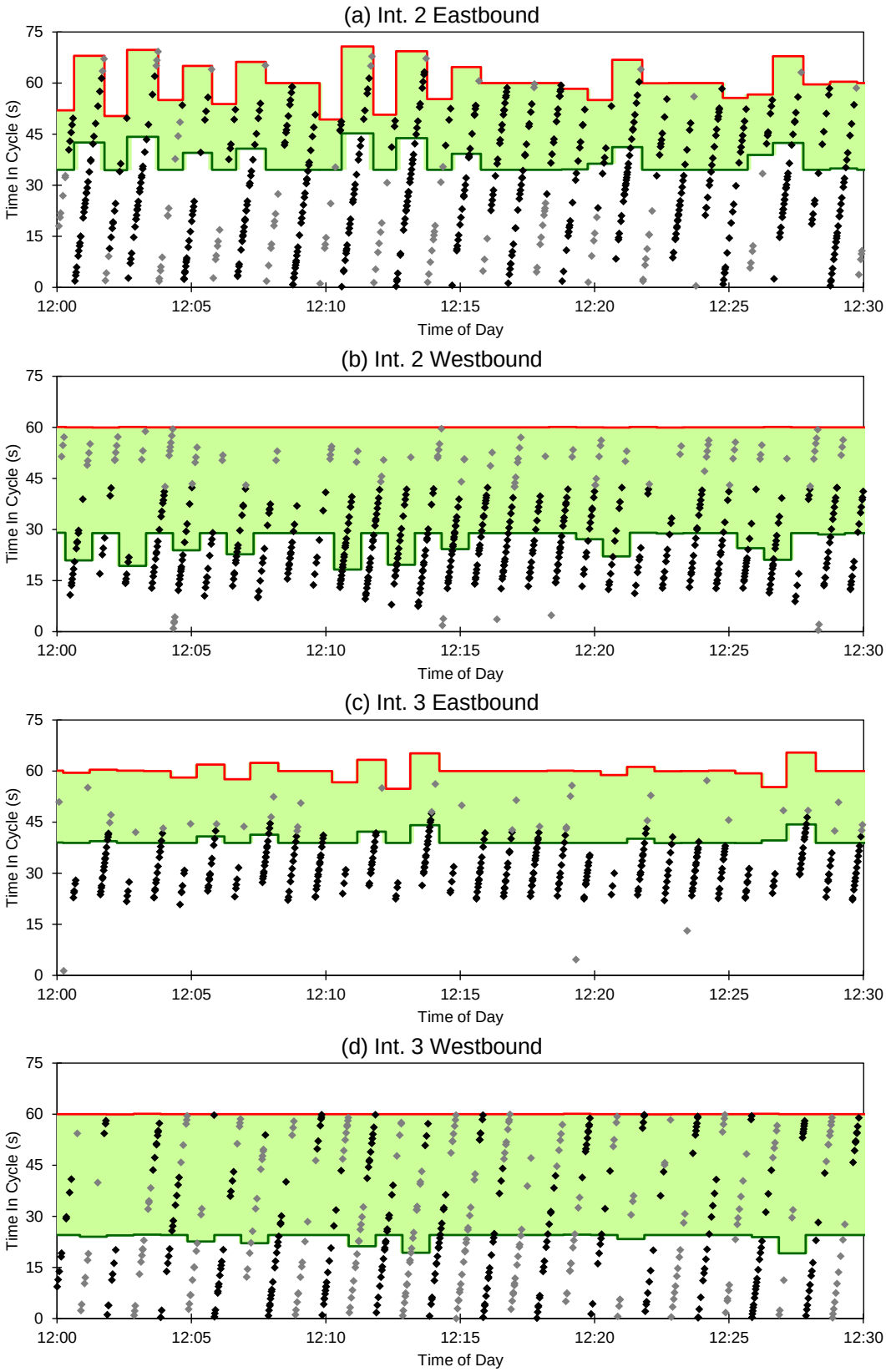

Figure 5. Detail of PCDs for approaches at the DDI crossover intersections.

- *Between Intersections 3 and 4*. This link is similar to the one spanning Intersections 1 and 2. Because of double cycling at Int. 3, Int. 4 eastbound (Figure 4g) receives four platoons per cycle: two platoons of through vehicles and two of upstream turning vehicles. Meanwhile, Int. 3 westbound (Figure 4h, Figure 5d) contains many vehicles originating from turning movements at Int. 4. Similar to Int. 2 eastbound, Int. 3 westbound has the appearance of random arrivals when viewing a long time period (Figure 4h) but focusing on a smaller duration reveals a two-cycle arrival pattern (Figure 5d).

- *Between Intersections 4 and 5*. This is the only link spanning two conventional intersections. Int. 5 eastbound has well-formed platoons (Figure 4i) while Int. 4 westbound (Figure 4h) appears almost random. There is relatively little platoon formation at the upstream intersection, which receives random arrivals and has very long green intervals. Vehicles turning in from the side street appear to completely fill in the gap between vehicles entering from the upstream through movement.

Adjusting Offsets with a Single-Controller Diamond

Single-controller diamonds have been extensively studied (*2,17,18*). Recently, techniques using high-resolution data to measure performance and optimize offsets in arterials (*14,19*) were applied to diamond interchanges (*15*), first to a conventional diamond (*16*) and later to a DDI (7). The focus of that research was to balance the offset between the two intersections within the diamond. The present study integrates those results with arterial offset optimization.

Figure 6 shows a time space diagram to help illustrate single-controller timing parameters can be converted to effective offsets and vice versa. Here, Int. 1 and 4 are conventional intersections, while Int. 2 and 3 are half-cycled diamond crossover intersections operated by Ring 1 and Ring 2 in a single-controller configuration. "Northbound" bands are shaded blue while "southbound" bands are shaded green. The offset values used to build each illustrations are shown on the left side of the figure.

Figure 6a shows initial conditions. The offset at each intersection is shown as O_1, O_2, etc.; offsets are defined as the displacement between the local zero[1] and the system zero. Subscripts *a,b,c,d* help compare values between scenarios. Note that O_3 is the *effective* offset at Int. 3; it is determined by the real-world parameters O_2 and ring displacement, R. The relationship between O_2, O_3, and R is

$$O_3 = (O_2 + R) \bmod C$$

where C is the cycle length. More generally, this can be written as

$$O_{[\text{Ring 2}]} = (O_{[\text{Ring 1}]} + R) \bmod C, \qquad \text{Equation 1}$$

where $O_{[\text{Ring1}]}$ and $O_{[\text{Ring2}]}$ are the offsets for the Ring 1 and Ring 2 intersections. Note that $O_{[\text{Ring1}]}$ is a real-world parameter, the offset for the interchange controller, while $O_{[\text{Ring2}]}$ is the effective offset of the Ring 2 intersection.

[1] The TS/2 definition of first coordinated green is used in this example, hence the local zero is associated with the earlier of Phase 2 or Phase 6.

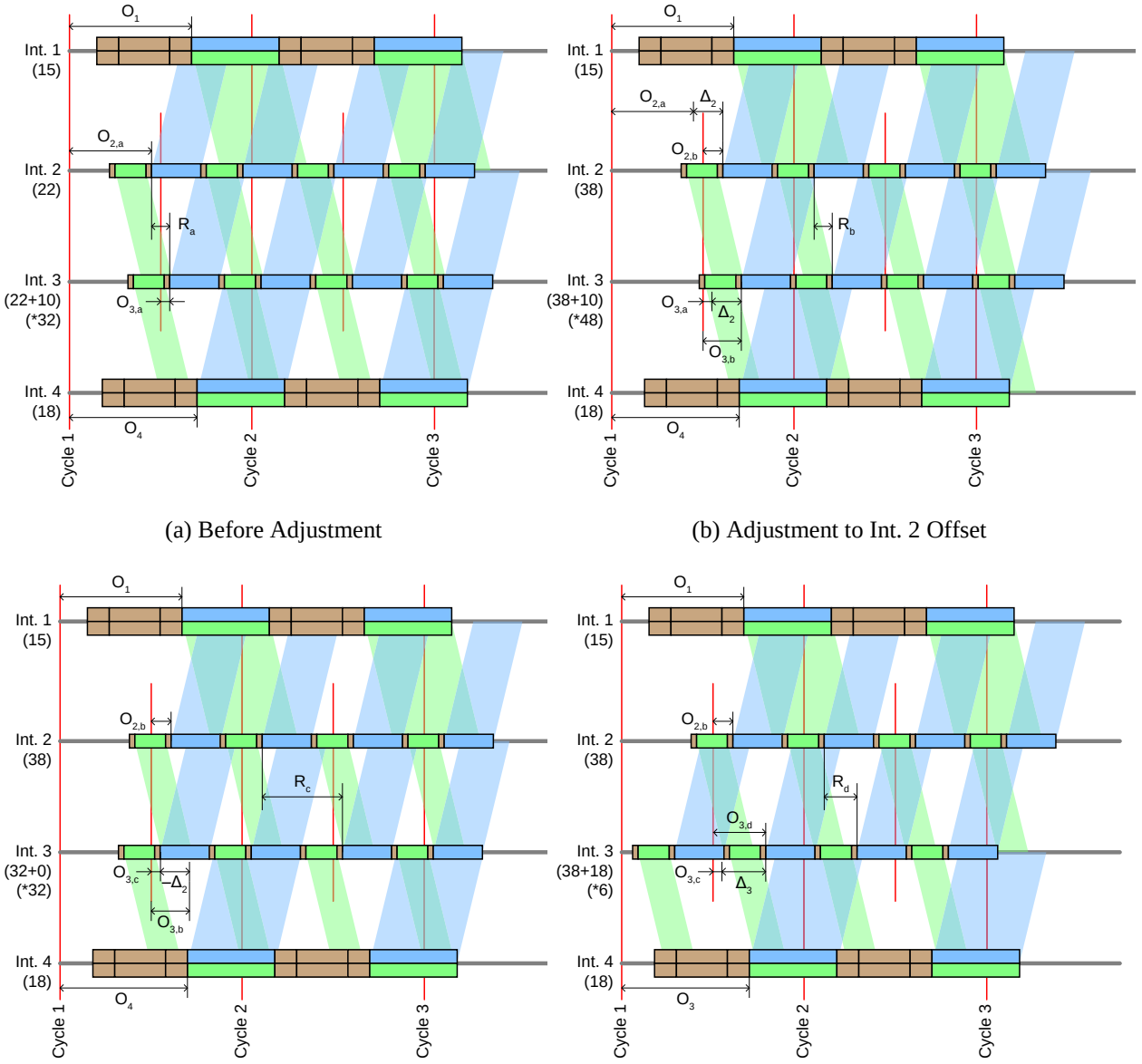

Figure 6. Relationship between coordination of two intersections operated by a single controller. Each intersection is labeled with the offset illustrated in each graphic. The label on Int. 3 shows the interchange offset plus ring displacement, such as (22+10), and the equivalent offset, such as (*32).

In Figure 6a, an adjustment to O_2 is made, shown as Δ_2. Because the adjustment applies to both rings, it also applies to O_3. Therefore the adjustments are:

$$\begin{cases} O_{2,b} = O_{2,a} + \Delta_2 \\ O_{3,b} = O_{3,a} + \Delta_2 \end{cases}$$

Note that the ring displacement is unchanged: $R_b = R_a$. To independently adjust O_2 without affecting O_3, Δ_2 would be subtracted from O_3. That scenario is shown in Figure 6c. The "decoupling" adjustment is:

$$O_{3,c} = O_{3,a} + \Delta_2 - \Delta_2 .$$

This returns O_3 to its initial value ($O_{3,a}$). The ring displacement is changed by doing so, with the resulting value

$$R_c = \left(R_a - \Delta_2\right) \bmod C .$$

Finally, consider an independent adjustment of O_3, as illustrated in Figure 6d. Here, Δ_3 is the independent adjustment for Int. 3,which is superimposed onto the previous adjustments, and is incorporated into the ring displacement as follows:

$$R_d = \left(R_c + \Delta_3\right) \bmod C$$
$$R_d = \left(R_a - \Delta_2 + \Delta_3\right) \bmod C$$

By converting between effective offsets and the real-world parameters, the two crossover intersections can be treated independently within any optimization model. A generalized formula for calculating a new ring displacement is

$$R_{\text{new}} = \left(R_{\text{old}} - \Delta_{[\text{Ring1}]} + \Delta_{[\text{Ring2}]}\right) \bmod C , \qquad \text{Equation 2}$$

where R_{old} and R_{new} are the old and new ring displacement values; and $\Delta_{[\text{Ring1}]}$ and $\Delta_{[\text{Ring2}]}$ are the desired adjustments to the effective offsets for the intersections controlled by Ring 1 or Ring 2. The offset adjustment for the interchange controller offset is simply $\Delta_{[\text{Ring1}]}$.

The new offset value for the interchange controller (and for updating offsets at the conventional intersections) is found by:

$$O_{\text{new}} = \left(O_{\text{old}} + \Delta\right) \bmod C , \qquad \text{Equation 3}$$

where O_{old} and O_{new} respectively are the old and new offsets and Δ is the adjustment.

Optimization Procedure

An offset optimization algorithm, described previously (*20*), was applied to optimize offsets along the corridor. This method uses an approach similar to TRANSYT (*21*), replacing modeled data with measured data. Offset adjustments are modeled by linear superposition of vehicle arrival times and green times (*14*). The algorithm performs these adjustments in a systematic fashion, similar to the Combination Method (*22*), with the objective of maximizing the arrivals on green (*19*). The resulting offset adjustments yielded by the procedure were then converted into new offsets and ring displacements using the methodology described in the previous section.

RESULTS

Arrivals on Green

New offsets were programmed on May 22, 2015. Bluetooth travel time monitoring was maintained on the corridor from May 14 to June 1, covering six pre-optimization and five post-optimization days. The Memorial Day holiday on May 25, 2015 was excluded from the analysis, as were weekends. The total number of arrivals along the corridor increased by about 6% between the "before" period and "after" period.

Figure 7 shows the PCDs for Wednesday, May 27, 2015 for the ten signalized approaches in the system from 6:00–18:30. These may be compared to the "before" PCDs in Figure 4 to assess operational changes. Some highlights of these include the following.

- *At the DDI*. Int. 3 Eastbound now has most of its arrivals coincident with the green band during all three timing plans (Figure 7e), whereas this was only true for the PM peak before optimization (Figure 4e). There are slight differences at Int. 2 westbound, which appear to have moved the ramp vehicles (gray dots) to the beginning of green (Figure 7d) whereas these arrived near the end of green previously (Figure 4d). While this was not done by design, the outcome is likely better for progression since most of the ramp vehicles are likely continuing through the intersection while many of the vehicles coming from the upstream arterial through movement (black dots) are likely turning onto the freeway.

- *Elsewhere*. For the most part, changes at the other approaches were relatively small in magnitude. Int. 1 westbound (Figure 7b) saw improved progression during the midday and PM peak. These were the most substantial improvements at a conventional interchange; this achieved the rather difficult situation of fitting multiple westbound platoons from the half-cycled upstream intersection within the local green band. Int. 4 eastbound (Figure 7g) has improved progression during the midday time period, but it is slightly worse during the PM peak. The AM peak is unchanged. Int. 4 westbound (Figure 7h) also worsened during the midday. Finally, Int. 5 eastbound (Figure 7i) had slightly worse midday progression but slightly better progression during the PM peak. Other approaches had relatively little change.

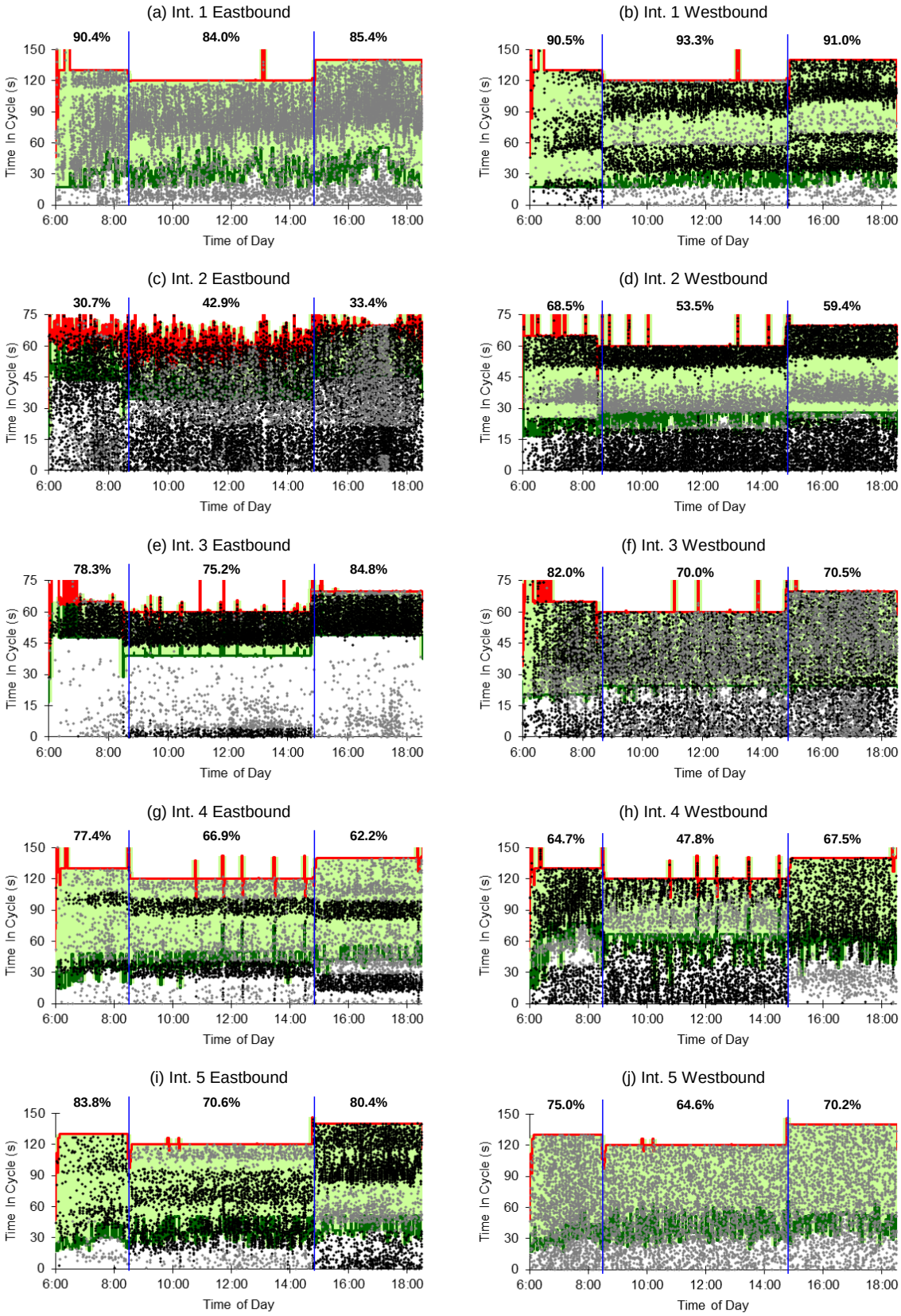

Figure 7. PCDs for Wednesday, May 27, 2015 (after optimization).

Changes in the percent on green (POG) at the ten coordinated approaches, averaged over 5 weekdays, are summarized by Figure 8. In general, there are more increases than decreases. Two notable increases occur on Eastbound at Int. 3 (Figure 8b). There were initially very few vehicles arriving on green in this movement before optimization, while after optimization the arrivals are aligned very well with the green. This led to improvements of over 60%. During the PM period, the existing timing had already captured those arrivals well, so a similar improvement is not seen for the PM.

There were several other improvements, such as for Int. 1 westbound during midday and PM; and Int. 4 eastbound during AM and midday. There were also reductions, such as Int. 4 westbound during midday and Int. 4 eastbound during the PM. These are attributable to tradeoffs in the optimization process that favored the opposing direction.

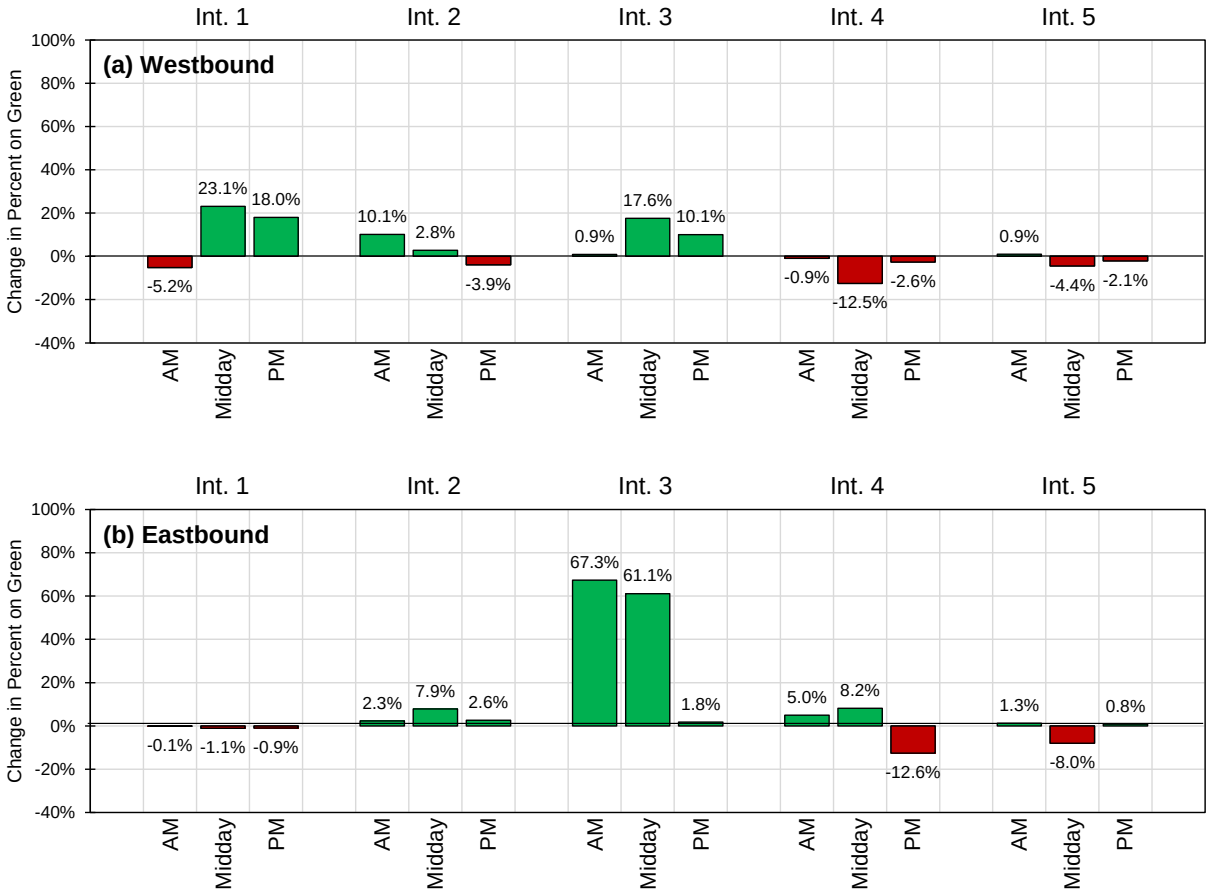

Figure 8. Change in Percent on Green: 5 weekdays before optimization versus 5 weekdays after optimization: a) Westbound and b) Eastbound.

Annualized User Costs

Figure 8 shows that the method for optimizing offsets achieves its goal of increasing POG. Changes in annualized user costs associated with travel times on various routes through the system are considered as a means of independently evaluating the impact of applying the optimization. The traditional approach to doing so is to consider arterial travel times using floating car studies, or more recently by using vehicle re-identification methods. This study not only considers end-to-end arterial travel times, but also considers several other important routes through the system and also considers the reliability of the travel times. The methodology follows an approach used in a recent study (*23*) to estimate user benefits from signal maintenance and optimization activities.

User benefits for the DDI retiming were estimated on the basis of individual origin-destination (O-D) pairs determined by the stationing of Bluetooth sensors in the network (Figure 1). It was necessary to estimate the total traffic volumes associated with each O-D pair. Rather than undertaking costly corridor instrumentation to derive comprehensive O-D estimates, several O-D paths derived from the Bluetooth data were compared against actual traffic counts from inductive loop detectors. This comparison was performed for different O-D pairs. From this, it was estimated that the Bluetooth measurements accounted for between 2% and 6% of total traffic volumes for individual O-D paths, with an average sample rate of 4%. Thus, total observed Bluetooth travel time counts were averaged by day for each O-D pair, and multiplied by 25 to determine an approximation of total daily traffic volumes. An adjustment factor from INDOT (*24*) was used to convert these estimates to AADT.

The following formula was used to convert the statistical properties of the measured travel times to annualized user costs (*c*):

$$c = \frac{364}{60} \cdot (T_{avg} v_{pc} o_{pc} u_{pc} + k_{pc} T_{std} v_{pc} o_{pc} u_{pc} + T_{avg} v_{hv} u_{hv} + k_{hv} T_{std} v_{hv} u_{hv}) \qquad \text{Equation 4}$$

where T_{avg} and T_{std} are the average and standard deviation of the travel times (minutes) for a given O-D pair and scenario; v_{pc} and v_{hv} are the vehicle and heavy vehicle volumes, found by combining field measured volumes with INDOT vehicle classification data; u_{pc} and u_{hv} are the unit value of travel time for passenger cars and heavy vehicles (dollars per person-hour); o_{pc} is the average passenger car occupancy; and k_{pc} and k_{hv} are conversion factors for passenger cars and heavy vehicles that assign a value per unit of travel time standard deviation.

Values of u_{pc} = \$17.67/hr and u_{hv} = \$94.04/hr were taken from the latest version of the *Urban Mobility Report* (*25*). Applying the findings of an NCHRP study (*26*), a ratio of 1.0 for the value of a unit change in variability (reliability) to a unit change in actual travel time was selected (i.e., $k_{pc} = k_{vh} = 1.0$). It was assumed that $o_{pc} = 1.25$.

The results are shown in Figure 9 and Figure 10. Figure 9 shows the annualized hourly user costs before and after offset optimization, by O-D route and time of day. The costs are shown in terms of travel time (TT) and travel time reliability (TTR). Meanwhile, Figure 10 shows the decreases in annualized user costs by O-D route and time of day. Cost increases, representing disbenefits, are shown here as negative values. These represent changes in total costs for the entire time of day period.

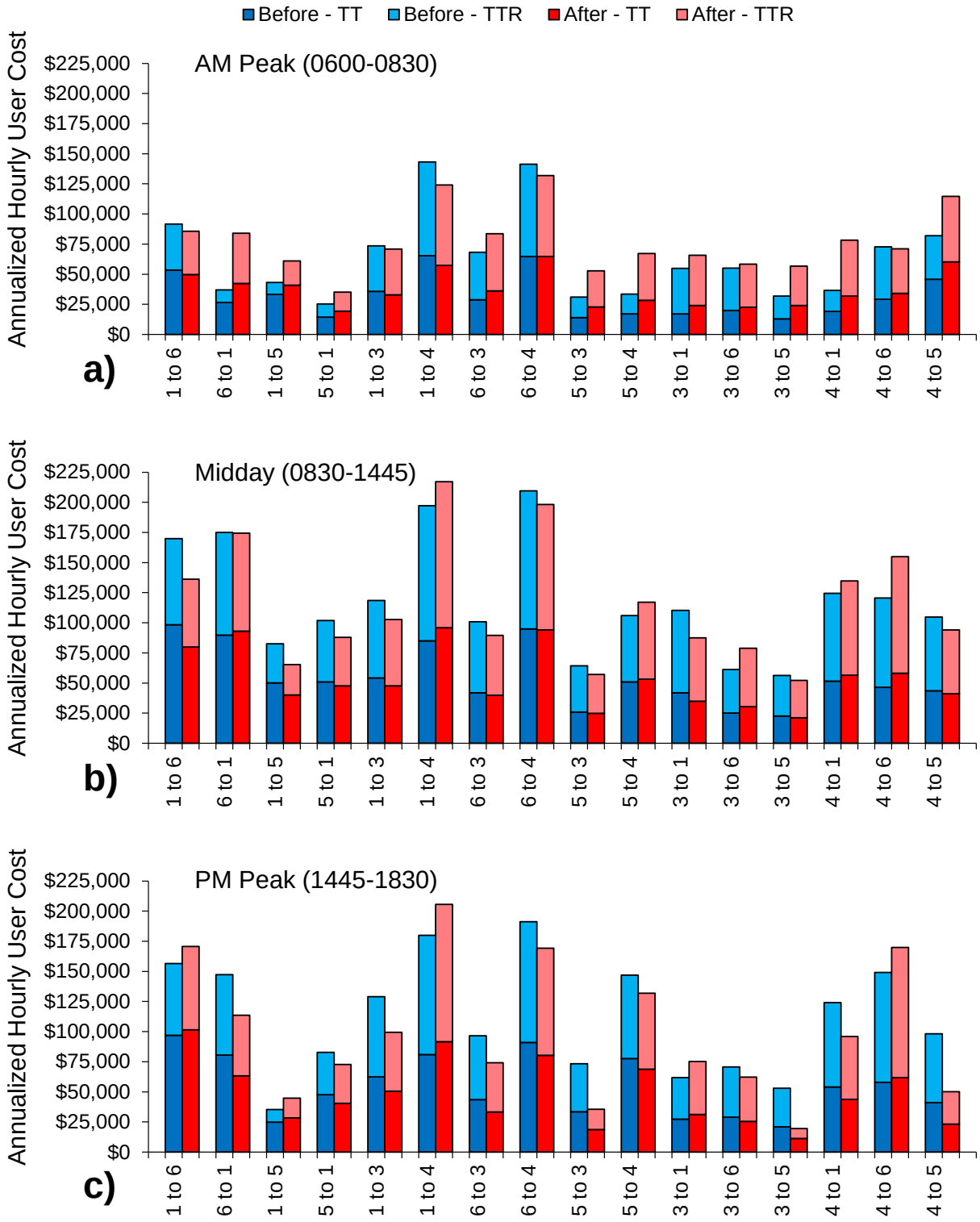

Figure 9. Total user cost per time of day period: a) AM peak; b) Midday; and c) PM Peak.

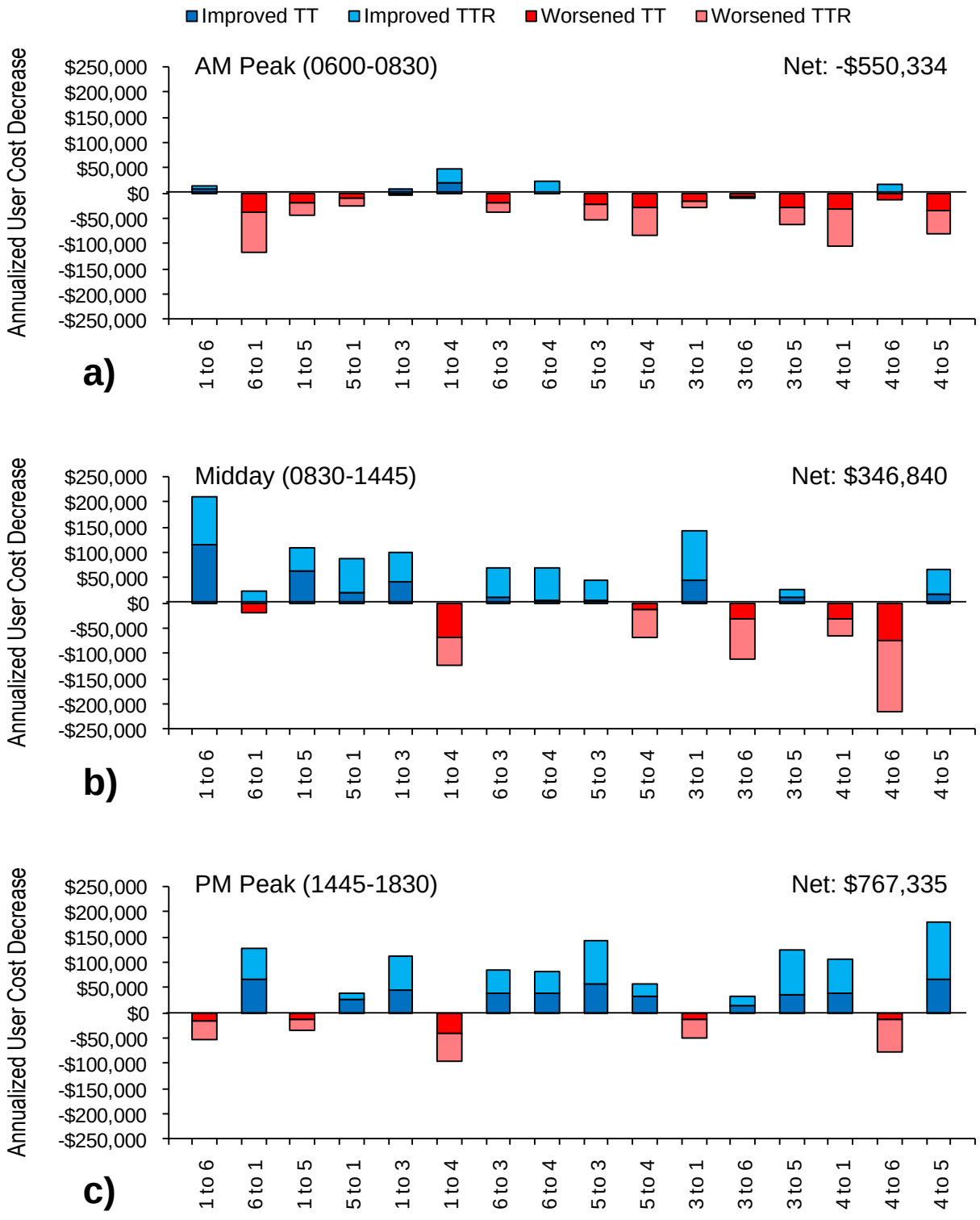

Figure 10. Changes in user cost per time of day period: a) AM peak; b) Midday; and c) PM Peak.

Total costs (Figure 9) vary considerably by time of day and route. Interestingly, the AM peak has the lowest costs per hour, which reflects that the actual peak occurs within a smaller portion of the 0600-0830 interval while during the other times of day the traffic is sustained throughout the time period. Also, the arterial routes (1 to 6 and 6 to 1) are not associated with the highest user costs. Routes leading to southbound I-65 (1 to 4 and 6 to 4) have that distinction. The return routes (4 to 1 and 4 to 6) also have high user costs. This reflects relatively high volumes for these routes.

Changes in user costs (Figure 10) vary considerably by time of day.

- The AM peak (Figure 10a) saw slight improvements for eastbound routes originating from the east end of the system, but the other routes mostly saw higher user costs, especially in the westbound direction. This seems to reflect the changes in POG (Figure 8), which saw eastbound increases and some westbound decreases. The eastbound volume is more dominant, which likely led the algorithm to value marginal improvements in eastbound progression more than the worsened westbound progression.
- The midday time period (Figure 10b) saw a better balance of improvements, with more routes having decreases in user costs than increases. Most of the arterial routes saw some improvements, with eastbound travel across the arterial (1 to 6) having the highest amount of improvement. Arterial routes heading toward southbound I-69 and routes from I-69 to the east end of the system saw worsened performance.
- Finally, the PM time period (Figure 10c) exhibited the greatest amount of improvement, with many different paths seeing decreases in user cost. For this time of day, westbound volumes are heavier than eastbound, which the result that nearly all of the westbound routes all see decreases in user costs, including both arterial and freeway origins and destinations. Most of the increases are associated with eastbound routes. This time period had the highest net user benefit.

The total estimated user benefit, found by summing the net benefit from each time period, was found to be approximately $564,000, after balancing user cost reductions of about $1,114,000 for the midday and PM peak time periods with a cost increase of about $550,000 associated with the AM period.

The objective of maximizing arrivals on green was successful, as shown by the increases in POG for most of the system (Figure 8). This yielded decreased travel times and user costs during the midday and PM time periods, which agrees with results seen in previous studies using the same general approach (*14*,*19*). As in those studies, the direction of travel with the dominant volume tends to determine which routes are more likely to see benefits. The AM peak, however, saw a net increase in user costs, which demonstrates that increased POG does not always directly translate to decreased travel time. While the dominant direction indeed saw some improvement, the cost increases were ultimately higher on the opposing routes. This result suggests that further exploration of alternative objective functions may be helpful. One possibility, which would likely be well-facilitated by O-D route based evaluation, would be optimization processes that consider O-D route performance directly. Such a method has been formulated for bandwidth optimization recently (*27*); it might be possible to integrate this concept with measured vehicle arrivals.

CONCLUSIONS

This paper presented a methodology for optimizing offsets on a corridor that included a single-controller DDI. This methodology enables the corridor to be modeled as a set of independent intersections, with the offset adjustments converted into the equivalent real-world single-controller offset and ring displacement parameters (Equation 2, Equation 3).

The methodology was applied to a 5-intersection arterial including a DDI (Figure 1). The impact of optimization was quantified in terms of annualized user costs based on measured travel time and travel time reliability across twelve O-D paths through the corridor. The amount of arrivals on green was increased for all time of day plans (Figure 8), and this translated into substantially reduced user costs for the midday and PM peak timing plans. The AM peak saw marginal improvements in the dominant direction, but yielded a net degradation of performance when considering multiple routes through the system, which demonstrates that there are opportunities to refine the optimization objectives. The overall results for the three time of day periods was found to be worth approximately $564,000 in user cost reductions based on travel time and travel time reliability measures.

While this methodology was applied to the example of a DDI, the same procedure could be used for other single-controller scenarios where ring displacement can be used. This would include conventional diamonds, TTI four-phase diamonds, continuous-flow intersections, displaced left turns, and so forth. Many of these schemes can be operated with multiple displaced rings in a single controller, facilitating independent operation, coordination, and eliminating communications issues. Future work would explore these applications further. The investigation of DDI operations incorporating pedestrian phases would also be considered in future research. The integration of phase sequence and two-phase versus three-phase operation (*7*) are additional topics for further study; some preliminary comparisons are described elsewhere (*9*).

Future work on this topic would repeat the process under different conditions to make the results more transferable, and would explore alternative optimization objectives further to better understand the interplay of localized progression improvements and O-D route travel time performance.

ACKNOWLEDGMENTS

The high-resolution signal event data in this study was acquired using Siemens m50 controllers. This work was supported in part by USDOT SBIR project (contract number DTFH61-14-C-00035) through Traffax, Inc. and the Joint Transportation Research Program administered by the Indiana Department of Transportation and Purdue University. The contents of this paper reflect the views of the authors, who are responsible for the facts and the accuracy of the data presented herein, and do not necessarily reflect the official views or policies of the sponsoring organizations. These contents do not constitute a standard, specification, or regulation.

REFERENCES

1. Chlewicki, G. New Interchange and Intersection Designs: The Synchronized Split-Phasing Intersection and the Diverging Diamond Interchange. Presented at the 2nd Urban Street Symposium, Anaheim, California, 2003.
2. Engelbrecht, R.J. and K.E. Barnes. Advanced Traffic Signal Control for Diamond Interchanges. *Transportation Research Record No. 1856*, 231-238, 2003.
3. *Missouri's Experience with a Diverging Diamond Interchange: Lessons Learned.* Report No. OR10-021, Missouri Department of Transportation, 2010.
4. Hu, P. *Advanced Signal Control Strategies and Analysis Methodologies for Diverging Diamond Interchanges.* PhD Thesis, University of Nevada Reno, 2013.
5. Yang, X., G.-L. Chang, and S. Rahwanji. Development of a Signal Optimization Model for Diverging Diamond Interchange. *Journal of Transportation Engineering*, Vol. 140(5), 04014010, 2014.
6. Tian, Z., H. Xu, G. de Camp, M. Kyte, and Y. Wang. Readily Implementable Signal Phasing Schemes for Diverging Diamond Interchanges. Presented at Transportation Research Board Annual Meeting, 2015.
7. Hainen, A.M., A.L. Stevens, C.M. Day, H. Li, J. Mackey, M. Luker, M. Taylor, J.R. Sturdevant, and D.M. Bullock. High-Resolution Controller Data Performance Measures for Optimizing Diverging Diamond Interchanges and Outcome Assessment with Drone Video. Presented at Transportation Research Board Annual Meeting, 2015.
8. Schroeder, B.J., K. Salamati, and J. Hummer. Calibration and Field Validation of Four Double-Crossover Diamond Interchanges in VISSIM Microsimulation. *Transportation Research Record No. 2404*, 49-58, 2014.
9. Day, C.M., A. Stevens, J.R. Sturdevant, and D.M. Bullock. Alternative Intersections and Interchanges Volume 2: Diverging Diamond Interchange Signal Timing. Final Report, SPR-3830, Joint Transportation Research Program, Indiana Department of Transportation, 2015.
10. Smaglik E.J., A. Sharma, D.M. Bullock, J.R. Sturdevant, and G. Duncan. Event-Based Data Collection for Generating Actuated Controller Performance Measures. *Transportation Research Record No. 2035*, 97-106, 2007.
11. Sturdevant, J.R. *et al*. *Indiana Traffic Signal High Resolution Data Logger Enumerations*. West Lafayette, Indiana, Purdue University, 2012. Available online at http://docs.lib.purdue.edu/jtrpdata/3/.
12. Bullock, D.M., C.M. Day, T.M. Brennan, J.R. Sturdevant, and J.S. Wasson. Architecture for Active Management of Geographically Distributed Signal Systems. *ITE Journal*, 81(5), 20-24, 2011.
13. Smith, W.B. *Signalized Corridor Assessment.* MS Thesis, Purdue University, 2014.
14. Day, C.M., R. Haseman, H. Premachandra, T.M. Brennan, J.S. Wasson, J.R. Sturdevant, and D.M. Bullock. Evaluation of Arterial Signal Coordination: Methodologies for Visualizing High-Resolution Event Data and Measuring Travel Time. *Transportation Research Record No. 2192*, 37-49, 2010.
15. Hainen, A.M. *Offset and Sequence Optimization of Signalized Diamond Interchanges Using High-Resolution Event-Based Data*. PhD Thesis, Purdue University, 2014.
16. Hainen, A.M., A.L. Stevens, R.S. Freije, C.M. Day, J.R. Sturdevant, and D.M. Bullock. High-Resolution Event-Based Data at Diamond Interchanges: Performance Measures and Optimization of Ring Displacement. *Transportation Research Record No. 2439*, 12-26, 2014.
17. Chaudhary, N.A. and C.-L. Chu. *Guidelines for Timing and Coordinating Diamond Interchanges with Adjacent Traffic Signals.* Report TX-00/4913-2, Texas Transportation Institute, 2000.
18. Nelson, E.J., D. Bullock, and T. Urbanik. Implementing Actuated Control of Diamond Interchanges. *Journal of Transportation Engineering*, 126, 390-395, 2000.

19. Day, C.M., T.M. Brennan, A.M. Hainen, S.M. Remias, H. Premachandra, J.R. Sturdevant, G. Richards, J.S. Wasson, and D.M. Bullock. Reliability, Flexibility, and Environmental Impact of Alternative Objective Functions for Arterial Offset Optimization. *Transportation Research Record No. 2259*, 8-22, 2011.
20. Day, C.M. and D.M. Bullock, Computational Efficiency of Alternative Algorithms for Arterial Offset Optimization. *Transportation Research Record No. 2259*, 37–47, 2011.
21. Robertson, D.I. *Transyt: a Traffic Network Study Tool*. Report LR 253, Road Research Laboratory, Crowthorne, Berkshire, UK, 1969.
22. Hillier, J.A. Appendix to Glasgow's Experiment in Area Traffic Control. *Traffic Engineering and Control* 7, 569-571, 1966.
23. Li, H., Lavrenz, S.M., Day, C.M., Stevens, A., Sturdevant, J.R., and Bullock, D.M. (2015) Quantifying benefits of signal timing maintenance using both travel time and travel time reliability measures. Transportation Research Board Annual Meeting, Washington, D.C., Paper No. 15-1343. Accepted for publication in *Transportation Research Record*; in press.
24. Indiana Department of Transportation. Latest INDOT Adjustment Factors. Available online at https://secure.in.gov/indot/files/INDOT_2013_AADT_Adjustment_Factors_Rev_20140814.pdf. Accessed July 31, 2015.
25. Schrank, D., Eisele, B., & Lomax, T. *2015 Urban Mobility Scorecard*. Texas A&M Transportation Institute, 2015.
26. Small, K., Noland, R., Chiu, X., & Lewis, D. *Valuation of Travel Time Savings and Predictability in Congested Conditions for Highway User-Cost Estimation*. NCHRP Report 431, TRB, 1999.
27. Arsava, T., Y. Xie, N. Gartner, and J. Mwakalonge. Progression Optimization Based on Vehicular Traffic Origin-Destination Data. Transportation Research Board Annual Meeting, Washington, D.C., Paper No. 15-5550.